



# HMGB1 Knockout Decreases Kaposi's Sarcoma-Associated Herpesvirus Virion Production in iSLK BAC16 Cells by Attenuating Viral Gene Expression

Su-Kyung Kang,<sup>a</sup> Yun Hee Kang,<sup>b</sup> Seung-Min Yoo,<sup>a</sup> Changhoon Park,<sup>a</sup> Hong Seok Kim,<sup>c</sup> Myung-Shin Lee<sup>a,b</sup>

<sup>a</sup>Department of Microbiology and Immunology, Eulji University School of Medicine, Daejeon, Republic of Korea

<sup>b</sup>Eulji Biomedical Science Research Institute, Eulji University School of Medicine, Daejeon, Republic of Korea

<sup>c</sup>Department of Molecular Medicine, College of Medicine, Inha University, Incheon, Republic of Korea

Su-Kyung Kang and Yun Hee Kang contributed equally to this work. Author order was determined alphabetically.

**ABSTRACT** Multiple host proteins affect the gene expression of Kaposi's sarcoma-associated herpesvirus (KSHV) during latent and lytic replication. High-mobility group box 1 (HMGB1) serves as a highly conserved chromosomal protein inside the cell and a prototypical damage-associated molecular pattern molecule outside the cell. HMGB1 has been shown to play a pathogenic role in viral infectious diseases and to regulate the lytic replication of KSHV. However, its functional effects on the KSHV life cycle in KSHV-infected cells have not been fully elucidated. Here, we explored the role of intracellular and extracellular HMGB1 in KSHV virion production by employing CRISPR/Cas9-mediated *HMGB1* knockout in the KSHV-producing iSLK BAC16 cell line. Intracellular HMGB1 formed complexes with various proteins, and the abundance of HMGB1-interacting proteins changed during latent and lytic replication. Moreover, extracellular HMGB1 was found to enhance lytic replication by phosphorylating JNK. Of note, the expression of viral genes was attenuated during lytic replication in *HMGB1* knockout iSLK BAC16 cells, with significantly decreased production of infectious virions compared to that of wild-type cells. Collectively, our results demonstrate that HMGB1 is an important cellular cofactor that affects the generation of infectious KSHV progeny during lytic replication.

**IMPORTANCE** The high-mobility group box 1 (HMGB1) protein has many intra- and extracellular biological functions with an intricate role in various diseases. In certain viral infections, HMGB1 affects the viral life cycle and pathogenesis. In this study, we explored the effects of *HMGB1* knockout on the production of Kaposi's sarcoma-associated herpesvirus (KSHV). *HMGB1* knockout decreased virion production in KSHV-producing cells by decreasing the expression of viral genes. The processes by which HMGB1 affects KSHV production may occur inside or outside infected cells. For instance, several cellular and viral proteins interacted with intracellular HMGB1 in a nucleosomal complex, whereas extracellular HMGB1 induced JNK phosphorylation, thereby enhancing lytic replication. Our results suggest that both intracellular and extracellular HMGB1 are necessary for efficient KSHV replication. Thus, HMGB1 may represent an effective therapeutic target for the regulation of KSHV production.

**KEYWORDS** CRISPR/Cas9, gene expression, HMGB1, herpesvirus, JNK signaling, KSHV, virus production

Kaposi's sarcoma-associated herpesvirus (KSHV), a member of the human herpesvirus family, causes Kaposi's sarcoma, primary effusion lymphoma, multicentric Castleman's disease, and KSHV inflammatory cytokine syndrome (1). Viruses reshape the intracellular

**Citation** Kang S-K, Kang YH, Yoo S-M, Park C, Kim HS, Lee M-S. 2021. *HMGB1* knockout decreases Kaposi's sarcoma-associated herpesvirus virion production in iSLK BAC16 cells by attenuating viral gene expression. *J Virol* 95:e00799-21. <https://doi.org/10.1128/JVI.00799-21>.

**Editor** Jae U. Jung, Lerner Research Institute, Cleveland Clinic

**Copyright** © 2021 American Society for Microbiology. All Rights Reserved.

Address correspondence to Hong Seok Kim, kimhs0622@inha.ac.kr, or Myung-Shin Lee, imslee@g.eulji.ac.kr.

**Received** 11 May 2021

**Accepted** 27 May 2021

**Accepted manuscript posted online** 2 June 2021

**Published** 26 June 2021

environment in host cells to amplify the production of viral progeny and subvert the anti-viral response. In fact, several KSHV proteins have been reported to interact with host cell proteins, while certain host proteins may play a critical role in the life cycle of KSHV (2–5).

High-mobility group box 1 protein (HMGB1) is a crucial chromatin protein. In the nucleus, HMGB1 organizes DNA and regulates transcription through interaction with nucleosomes, transcription factors, and histones (6). In addition, HMGB1 can be secreted from cells through the leaderless secretory pathway. Secreted HMGB1 acts as a cytokine mediator of inflammation by binding to the receptor for advanced glycation end products (RAGE) and Toll-like receptors (TLRs) (7). As a result, HMGB1 activates components of downstream signaling pathways, including those associated with NF- $\kappa$ B (8), mitogen-activated protein kinases (MAPKs) (9), and phosphoinositide 3-kinase (10), thereby modulating inflammatory responses and promoting cell proliferation, angiogenesis, cell adhesion, and migration.

Several reports have suggested that HMGB1 affects viral life cycles, as it is upregulated in host cells following infection with certain viruses, including Epstein-Barr virus (11) and human T-cell lymphotropic virus type 1 (12). In virus-infected cells, HMGB1 affects cellular functions and virus replication. Hepatitis B virus X protein has been reported to bind to HMGB1, triggering autophagy in hepatocytes (13). Additionally, HMGB1 binds to the nucleoprotein component of influenza virus ribonucleoprotein and enhances the transcription/replication activity of the viral polymerase (14). With respect to KSHV, a previous study demonstrated that HMGB1 enhances KSHV replication and transcription activator (RTA) binding to the RTA-responsive elements of KSHV target genes (15). Furthermore, Harrison and Whitehouse reported that HMGB1 binds and synergistically upregulates the KSHV *ORF50* promoter in conjunction with RTA (16). Although the role of HMGB1 in the KSHV life cycle was suggested in these previous studies, the broad functional effects of HMGB1 on the KSHV life cycle in KSHV-infected cells have remained relatively unexplored. In particular, little is known about extracellular HMGB1 expression and its modulatory effect on KSHV-producing cells.

In the present study, we investigated the role of HMGB1 in the KSHV life cycle using KSHV-producing iSLK BAC16 cells with CRISPR/Cas9-mediated *HMGB1* knockout (KO). Our results revealed that HMGB1 participates in the production of KSHV in multiple ways, suggesting that it affects the pathogenesis of KSHV-mediated diseases.

## RESULTS

**Expression of HMGB1 in KSHV-producing iSLK BAC16 cells.** HMGB1 is a crucial cellular molecule required for the replication of several viruses, including severe acute respiratory syndrome coronavirus 2 and human immunodeficiency virus 1 (17, 18). Additionally, HMGB1 reportedly affects the life cycle of KSHV (15, 16); however, its precise role in a KSHV-producing cell line has not been fully elucidated. Thus, here we knocked out *HMGB1* in KSHV-producing iSLK BAC16 cells to investigate the effect of HMGB1 on viral progeny production. However, during the CRISPR/Cas9-mediated knockout process, isolation of a single cell clone by limiting dilutions is required, which can result in cellular heterogeneity that complicates the interpretation of the results. Therefore, to circumvent this issue, a single clone was isolated from the KSHV-carrying iSLK BAC16 cells before CRISPR/Cas9-mediated knockout, which was then used for further experiments. Analysis of HMGB1 expression in the isolated clone of iSLK BAC16 cells is illustrated in Fig. 1. To stimulate reactivation of KSHV, lytic replication was induced via treatment of iSLK BAC16 cells with doxycycline and sodium butyrate. Similar amounts of HMGB1 were detected in the whole-cell lysates from both latent and reactivated iSLK BAC16 cells by Western blotting (Fig. 1A). In the immunofluorescence assay (IFA), a strong signal for HMGB1 was detected in the nucleus, whereas in the cytoplasm, HMGB1 was not observed unless lytic replication was induced (Fig. 1B). While HMGB1 was strongly expressed in the nucleus upon lytic replication, only a weak signal was detected in the cytoplasm (white arrows in Fig. 1B). These results indicate that the induction of lytic replication of KSHV prompted the translocation of HMGB1

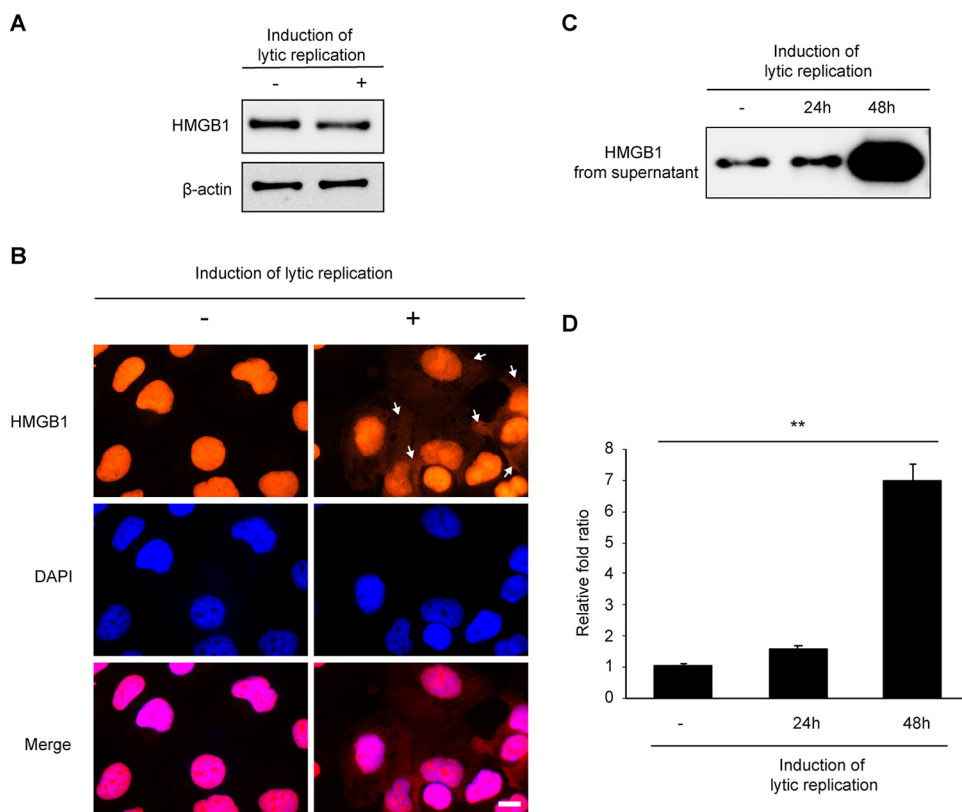


**FIG 1** HMGB1 expression in KSHV-producing iSLK BAC16 cells. (A) HMGB1 expression in iSLK BAC16 cells. Cell lysates were prepared from iSLK BAC16 cells with or without induced lytic replication, and HMGB1 expression was analyzed by Western blotting. (B) HMGB1 expression in iSLK BAC16 cells was visualized by the immunofluorescence assay (red color); nuclei were stained with DAPI (blue color). Cytoplasmic HMGB1 was indicated by white arrows. Scale bar, 10  $\mu$ m. (C) The release of HMGB1 into the extracellular space by iSLK BAC16 cells. Supernatants were collected from iSLK BAC16 cells without lytic replication (–) or 24 or 48 h after lytic replication induction. The culture supernatants were concentrated using Amicon Ultra centrifugal filters (molecular weight [MW], 10,000) and analyzed by Western blotting. (D) Densitometry analysis of HMGB1 expression in the supernatant. Statistical significance of differences is indicated as follows: \*\*,  $P < 0.01$ , one-way ANOVA test.

from the nucleus to the cytoplasm, which may have induced the extracellular release of HMGB1 from reactivated KSHV-infected cells. To determine if extracellular HMGB1 is released by iSLK BAC16 cells, we collected the supernatant from iSLK BAC16 cell cultures with or without reactivation (Fig. 1C and D). In the absence of reactivation, extracellular HMGB1 from iSLK BAC16 cells was detected as a clear band in Western blotting. After reactivation, a significant increase in the abundance of HMGB1 was observed in the supernatant over time. Similar results, demonstrating the release of HMGB1 from virus-infected cells, have been reported in different virus-infected cells, including other herpesviruses (19–22). Our results demonstrated that HMGB1 was secreted from iSLK BAC16 cells even without induction of lytic replication and that a larger amount of HMGB1 could be released after iSLK BAC16 cell reactivation.

**Knockout of *HMGB1* in iSLK BAC16 cells.** A ribonucleoprotein complex consisting of the Cas9 protein and *HMGB1*-targeting guide RNA (gRNA) was transfected into iSLK BAC16 cells to knock out *HMGB1*. Each clone was then separated using the limiting dilution technique, and HMGB1 expression was analyzed by Western blotting to isolate a knockout (KO) clone (data not shown). To confirm the KO of *HMGB1*, we used a PCR-based genotyping method to detect the genetic mutation. One pair of the primers was designed outside the Cas9 cutting site (primers F and R), while the other targeted the Cas9 cutting site (primer S; Fig. 2A). Thus, HMGB1-FR can amplify both wild-type (WT) and mutant alleles, while HMGB1-SR amplifies WT alleles. Thus, any newly acquired

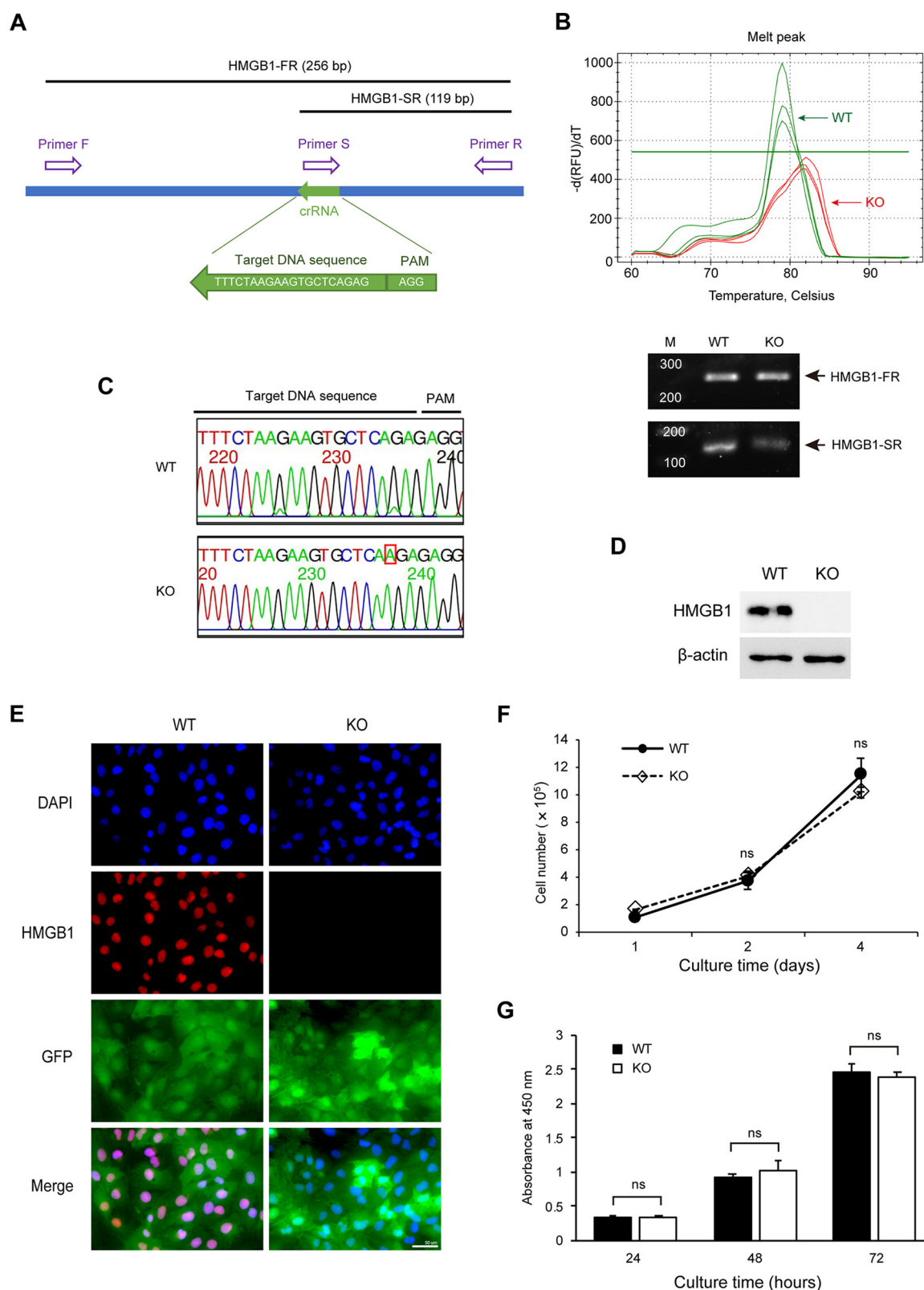


**FIG 2** Knockout of *HMGB1* in iSLK BAC16 cells. iSLK BAC16 cells were treated using the CRISPR/Cas9 system and gRNA against *HMGB1*. The isolated clone with a knockout (KO) of *HMGB1* was analyzed for *HMGB1* sequence, *HMGB1* protein expression, and cell proliferation. (A) Schematic diagram showing primers for detecting mutations in the Cas9 targeting site of *HMGB1*. The synthetic primers for PCR amplification and CRISPR/Cas9 crRNA are indicated in purple and green, respectively. (B) Analysis for quantitative PCR for *HMGB1* wild type (WT) and KO clone with designed primers. Melting curve analysis (upper) in qPCR with triplicate samples and

(Continued on next page)

mutations disrupt amplification of the HMGB1-SR. Quantitative PCR (qPCR) results for WT and KO clones revealed different melting peaks, with fewer amplified PCR products detected for the KO clone than for the WT clone (Fig. 2B).

To generate single-copy mutant DNA fragments for subsequent sequencing, we cloned the PCR products generated from HMGB1-FR into a T-cloning vector, resulting in 10 colonies that were analyzed using conventional sequencing analysis. Theoretically, as the human genome has two alleles, two different mutants were expected. However, all colonies exhibited the same mutation with an additional A insertion in the Cas9 targeting site (Fig. 2C). These results suggest that both alleles harbor the same mutation. However, the possibility that only one allele was detected in an analysis using only 10 colonies cannot be excluded.

HMGB1 expression in a WT and KO iSLK BAC16 clone was analyzed by Western blotting and IFA (Fig. 2D and E). KSHV BAC16-infected cells express green fluorescence protein (GFP) due to the presence of a GFP cassette in these cells. Despite the ablation of HMGB1, the cellular morphology and proliferation of KO clones were not significantly affected compared to those of WT cells (Fig. 2E to G).

**Cellular and viral gene expression profiling in *HMGB1* knockout iSLK BAC16 cells.** RNA isolates were prepared from WT and *HMGB1* KO iSLK BAC16 cells in the absence of, or following, reactivation. Gene expression profiles in *HMGB1* KO iSLK BAC16 cells were analyzed from two independent experiments using *Homo sapiens* transcriptome sequencing. A gene with  $\geq 2$ - or  $\leq 0.5$ -fold difference in expression levels between WT and *HMGB1* KO extracts was considered differentially expressed. In both latent and reactivated cells, gene expression profiles were affected by the KO of *HMGB1* (Fig. 3). In particular, the induction of lytic replication caused significant changes in the expression of 1,025 genes (502 upregulated and 522 downregulated) in *HMGB1* KO iSLK BAC16 cells compared with WT controls. The 1,025 genes were clustered by hierarchical clustering to create a heatmap (Fig. 3A) and analyzed to identify pathways enriched in ontology clusters using Metascape gene list analysis (Fig. 3B). This analysis revealed glucocorticoid receptor pathway, Hedgehog signaling pathway, transmembrane receptor protein tyrosine kinase signaling pathway, calcium signaling pathway, p53 transcriptional gene network, Hippo signaling pathway, positive regulation of G protein-coupled receptor signaling pathway, positive regulation of STAT cascade, negative regulation of multicellular organism growth, regulation of fibroblast growth factor receptor signaling pathway, adenylate cyclase-activating G protein-coupled receptor signaling pathway, regulatory circuits of the STAT3 signaling pathway, and Hippo-Merlin signaling dysregulation as the processes predominantly affected by *HMGB1* KO in reactivated iSLK BAC16 cells.

In addition, the expression of 72 microRNAs (miRNAs) was significantly ( $\geq 1.5$ -fold) altered in reactivated *HMGB1* KO cells compared to those in control cells (36 miRNAs were upregulated and 36 miRNAs were downregulated). These miRNAs were clustered by hierarchical clustering to create a heatmap (Fig. 3C), and Metascape gene list analysis revealed that pathways associated with gene silencing by miRNA, negative regulation of sprouting angiogenesis, negative regulation of cell differentiation, negative regulation of biological process, cell proliferation, and signaling were particularly sensitive to *HMGB1* KO in reactivated iSLK BAC16 cells. Taken together, our results indicated that HMGB1 regulates not only the expression of mRNAs but also that of miRNAs in iSLK BAC16 cells.

Under the same conditions, 86 KSHV genes with altered expression were clustered by hierarchical clustering to create a heatmap (Fig. 3D). In the latent state, the expression of LANA was downregulated in *HMGB1* KO cells compared to WT cells. Moreover, induction of lytic replication upregulated the expression of many KSHV genes in both WT and

## FIG 2 Legend (Continued)

representative PCR products in gel electrophoresis (lower) is shown. (C) *HMGB1* sequence analysis in WT and KO iSLK BAC16 cells. The HMGB1-FR PCR products from WT and KO clones were cloned into T-vector, and the sequences were analyzed by conventional sequencing from 10 colonies. The nucleotide inserted into the CRISPR/Cas9 target site of *HMGB1* in the KO clone is indicated in a red box. (D) Western blotting of HMGB1 expression in WT and *HMGB1* KO cells. (E) Immunofluorescence assay of HMGB1 expression. Scale bar, 50  $\mu$ m. (D and E) Proliferation of WT and *HMGB1* KO iSLK BAC16 cells. At each time point, live cells were analyzed by trypan blue exclusion (D) and WST-1 viability testing (E). Statistical significance of differences is indicated. ns, not significant, Student's *t* test.

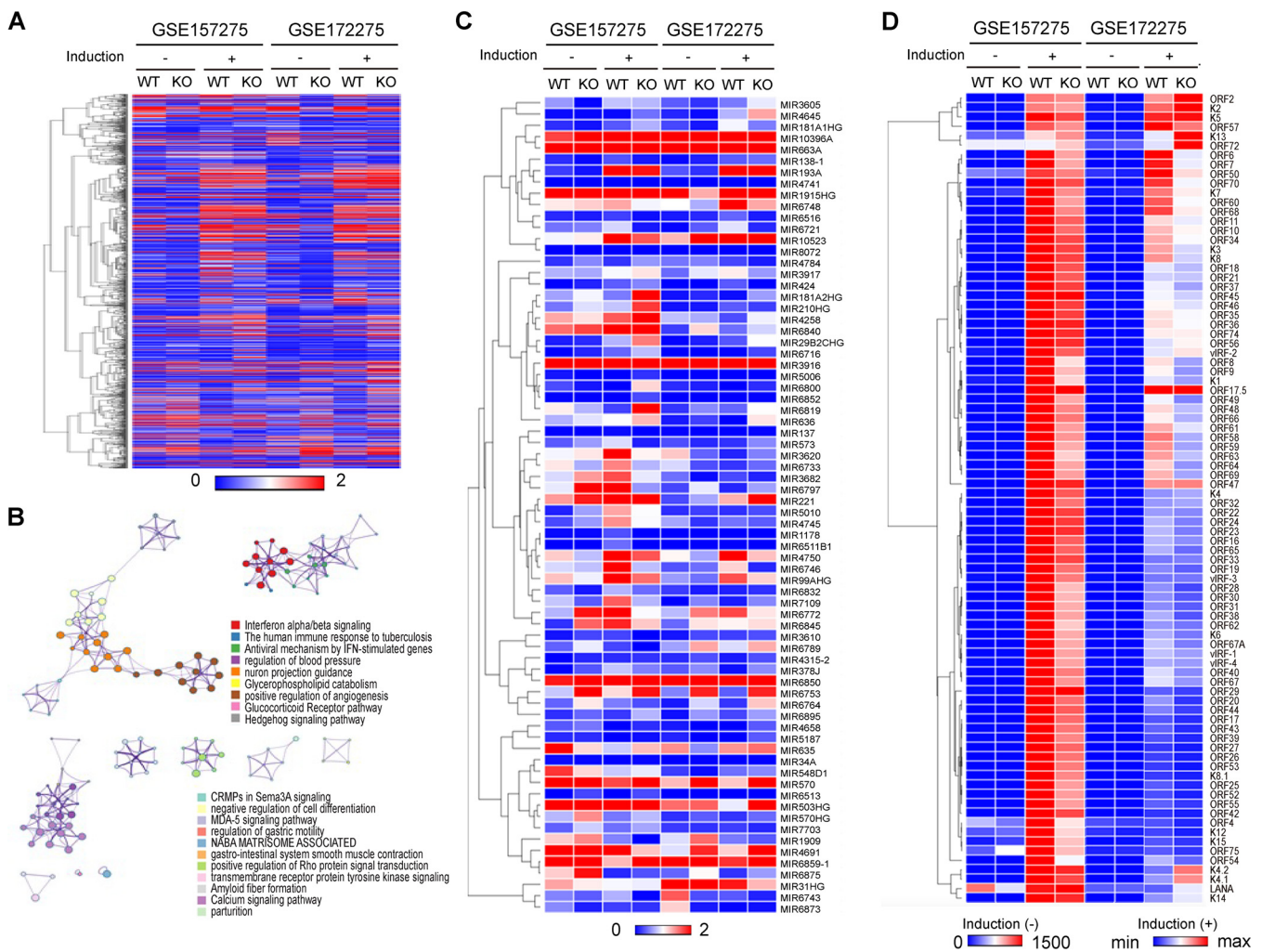


**FIG 3** Analysis of expression of host cell genes and miRNA as well as KSHV genes in *HMGB1* knockout iSLK BAC16 cells. The transcriptomes of wild-type (WT) and *HMGB1* knockout (KO) cells were analyzed by mRNA-seq. (A) Hierarchical cluster map of gene expression levels in *HMGB1* WT versus KO iSLK BAC16 cells with (induction +) or without (induction -) KSHV lytic replication. (B) Metascap pathway analysis of enriched ontology clusters of mRNA-seq results showed the top 20 pathways affected in the reactivated *HMGB1* KO cells compared to WT cells. (C) Hierarchical cluster map of miRNA expression levels for *HMGB1* WT versus KO iSLK BAC16 cells with (induction +) or without (induction -) KSHV lytic replication. (D) Heatmap of KSHV viral mRNA expression levels of *HMGB1* WT versus KO iSLK BAC16 cells, with (induction +) or without (induction -) KSHV lytic replication.

*HMGB1* KO cells. However, most viral genes were underexpressed in *HMGB1* KO cells compared to WT cells, suggesting that *HMGB1* regulates KSHV gene expression during both latent and lytic replication.

**Alteration of expression of KSHV genes by *HMGB1* knockout.** To validate the differential expression profiles of viral genes obtained by transcriptome sequencing (RNA-seq) analysis, quantitative reverse transcription-PCR (RT-qPCR) was performed on nine selected KSHV genes in WT and *HMGB1* KO iSLK BAC16 cells (Fig. 4A). Upon induction of lytic replication, the transcript level of KSHV *ORF73*, a latent gene, increased over time. Although KSHV *ORF73* expression was also increased in *HMGB1* KO cells during lytic replication, it was significantly lower than that in WT cells. Furthermore, the mRNA expression levels of the immediately-early (*ORF50*), early (*ORF59*, *K8*, and *ORF74*), and late lytic KSHV genes (*ORF65* and *K8.1*) were also significantly underexpressed in *HMGB1* KO cells compared to those in WT cells. Intriguingly, the mRNA expression of *ORF72* and *K13* was increased in KO cells compared to that in WT cells during induction of lytic replication, which was consistent with RNA-seq analysis. Western blotting of KSHV proteins further demonstrated results that were consistent with the quantitative RT-PCR data (Fig. 4B). After reactivation, all analyzed viral proteins

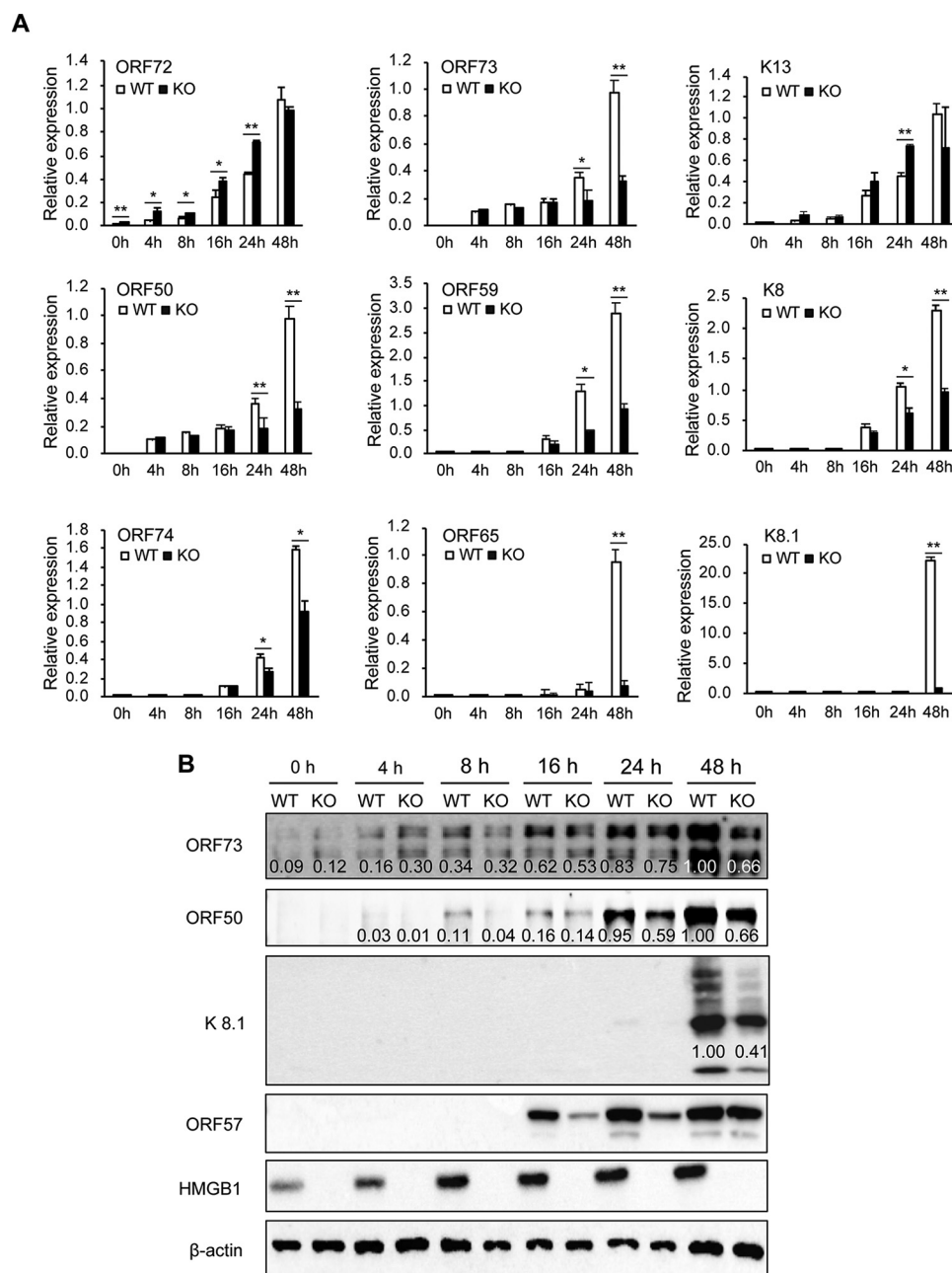


**FIG 4** KSHV gene expression in *HMGB1* knockout iSLK BAC16 cells. KSHV gene expression was analyzed in *HMGB1* knockout (KO) and wild-type (WT) iSLK BAC16 cells after the induction of lytic replication. (A) Relative mRNA expression levels of KSHV *ORF72*, *ORF73*, *K13*, *ORF50*, *ORF59*, *K8*, *ORF74*, *ORF65*, and *K8.1* determined by quantitative RT-PCR. Statistical significance of differences is indicated: \*,  $P < 0.05$ ; \*\*,  $P < 0.01$ , Student's *t* test. (B) KSHV *ORF73*, *ORF50*, *K8.1*, and *ORF57* protein expression levels determined by Western blot analysis. The indicated numbers are densitometric values for each of the target protein bands, which were normalized by the beta-actin signal.

were detected in *HMGB1* KO iSLK BAC16 cells; however, their expression levels were lower than those in WT cells. The expression levels of viral proteins (KSHV *ORF73* and *ORF50*) from WT and *HMGB1* KO cells correlated with their mRNA expression, suggesting that *HMGB1* enhanced viral protein expression during KSHV reactivation through the regulation of viral mRNA expression.

**HMGB1 participates in nucleosomal remodeling during the reactivation of KSHV.** KSHV lytic replication can be initiated by the expression of the *ORF50*-encoded immediate-early protein RTA (23). KSHV RTA reportedly forms a nucleosome complex

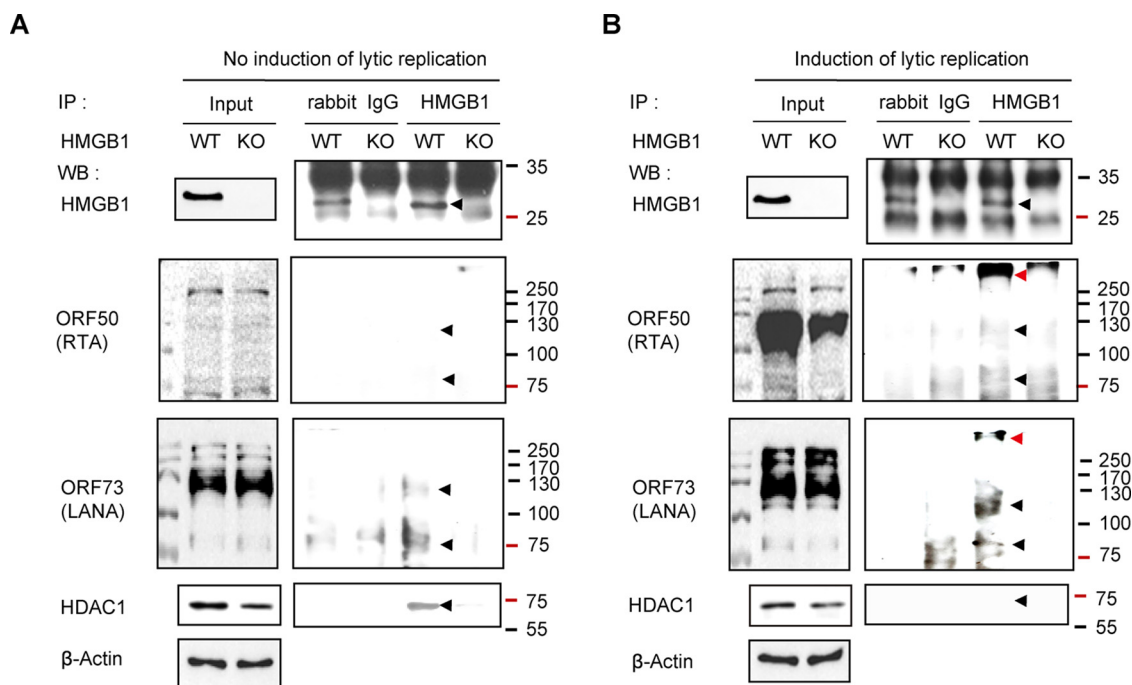


**FIG 5** Nucleosomal remodeling with HMGB1 in iSLK BAC16 cells with or without reactivation of lytic replication. Cell lysates prepared from wild-type (WT) or *HMGB1* knockout (KO) iSLK BAC16 cells were precipitated with an anti-HMGB1 antibody. Rabbit IgG was used as a negative control for precipitation. The precipitated proteins were analyzed by immunoblotting with anti-HMGB1 antibody, anti-KSHV ORF50 antibody, anti-KSHV ORF73 antibody, anti-HDAC1 antibody, and anti-β-actin antibody. Data for the HMGB1-interacting proteins are shown for iSLK BAC16 cells in the absence of lytic replication (A) or upon the induction of lytic replication (B). The expected protein sizes are indicated by black arrows. The bands thought to be complex forms with other proteins were indicated with red arrows.

with several host cell proteins in the immediate-early promoter region (23). Histone deacetylases (HDACs) are associated with the nucleosome complex and contribute to the stable repression of RTA, whereas histone acetylation caused by sodium butyrate triggers nucleosome remodeling and activation of RTA transcription (24). A previous study showed that the KSHV RTA and HMGB1 complex transactivates the KSHV *ORF50* promoter (16). Thus, to confirm that HMGB1 participates in the nucleosome complex in iSLK BAC16 cells, HMGB1-interacting proteins were analyzed by immunoprecipitation (Fig. 5). RTA was not detected in iSLK BAC16 cells with latent infection (Fig. 5A), whereas immunoprecipitated RTA protein was observed in reactivated WT cells (Fig. 5B). We also confirmed that HMGB1 interacts with the ORF73 protein (Fig. 5A and B), which was consistent with the results of a previous study (25). The interaction between HDAC1 and HMGB1 was detected during latent replication. However, after reactivation, the HDAC1 protein was not observed in HMGB1 immunoprecipitants. These results are consistent with the previous results reported for nucleosome modification during KSHV reactivation (24). In *HMGB1* KO iSLK BAC16 cells, neither protein was coimmunoprecipitated with HMGB1. Taken together, our results indicate that HMGB1 forms a nucleosome complex with viral and host proteins in iSLK BAC16 cells. Thus, considering that HMGB1 was previously reported to facilitate RTA-mediated expression of KSHV genes (15), it is plausible that HMGB1 in complex with viral and host cell proteins in the nucleosome regulates viral gene expression during the reactivation process by nucleosome remodeling.

**HMGB1 induces RTA-related signaling pathways.** In addition to its intracellular role as a nuclear cofactor for transcription regulation, HMGB1 performs extracellular functions after its release from cells. Extracellular HMGB1 activates multiple signaling pathways, e.g., mitogen-activated protein kinase (MAPK) and NF-κB, by binding to specific receptors, such as RAGE and TLRs (26). Certain specific signaling pathways, such as

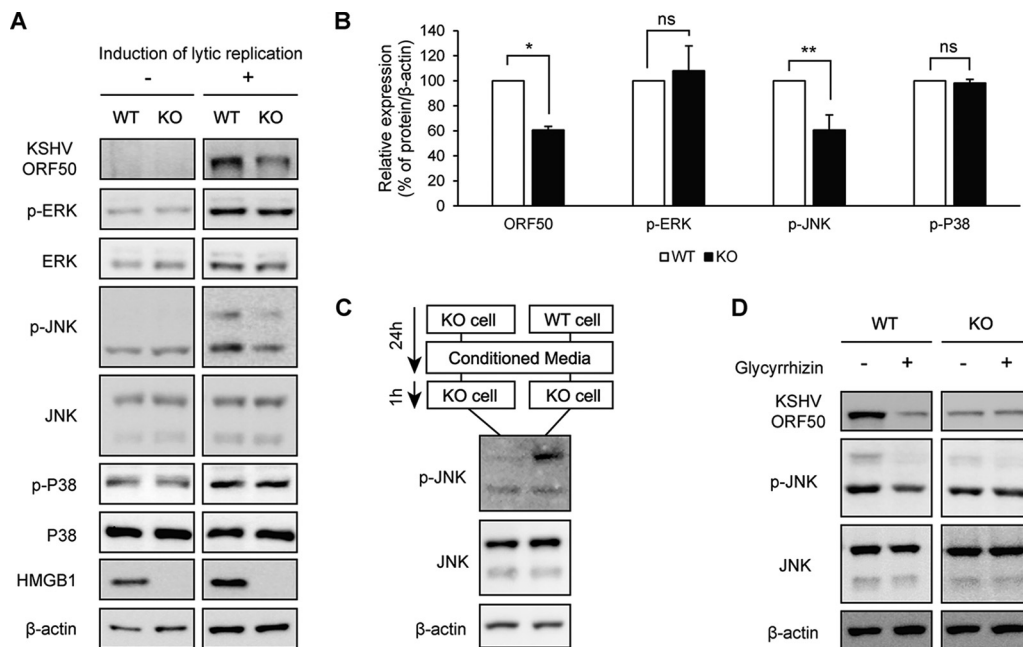


**FIG 6** Suppression of signaling pathways by *HMGB1* knockout. (A and B) Changes in the levels of activation of p38, JNK, and ERK in *HMGB1* knockout (KO) iSLK BAC16 cells. (A) At 48 h after the induction of lytic replication, protein lysate was collected and protein expression was analyzed using Western blotting in wild-type (WT) and *HMGB1* knockout (KO) iSLK BAC16 cells. (B) The results of Western blotting are presented as densitometric analysis. (C) The conditioned media from WT iSLK BAC16 cells induced phosphorylation of JNK. The supernatant from WT or *HMGB1* KO iSLK BAC16 cells was used to treat *HMGB1* KO iSLK BAC16 cells for 1 h, after which p-JNK was analyzed by Western blot analysis. (D) Lytic replication of KSHV was suppressed in WT and *HMGB1* KO iSLK BAC16 cells by glycyrrhizin. At 48 h after the induction of lytic replication, with or without glycyrrhizin, cell lysates were collected, and protein expression was analyzed by Western blotting. DMSO was used as a vehicle control.

MEK/ERK, JNK, and p38 MAPK pathways, enhance KSHV reactivation by activating the RTA promoter (27–29).

To investigate the relationship between these signaling events and HMGB1, we compared the activity levels of the MEK/ERK, JNK, and p38 MAPK pathways in WT and *HMGB1* KO iSLK BAC16 cells during the reactivation process (Fig. 6A). Results show that while the phosphorylation (p-) of ERK and p38 was similar between WT and KO cells after induction of lytic replication, p-JNK suppression was observed in the KO cells compared to WT cells (Fig. 6A and B). As shown in Fig. 1C and D, iSLK BAC16 cells released HMGB1 into the extracellular medium, causing the level of extracellular HMGB1 to increase after reactivation. Given that extracellular HMGB1 can activate JNK by binding to RAGE (30, 31), the difference in the expression levels of p-JNK in the *HMGB1* KO and WT cells may be attributed to the action of extracellular HMGB1. Therefore, the conditioned medium from WT or *HMGB1* KO cells was used to treat KO cells to investigate effects on JNK phosphorylation (Fig. 6C). We found that p-JNK was highly upregulated in cells treated with conditioned medium derived from WT cells compared to those treated with medium derived from KO cells.

To confirm that HMGB1 affects these signaling cascades and the lytic replication of KSHV, iSLK BAC16 cells were treated with the HMGB1 inhibitor glycyrrhizin. Glycyrrhizin suppressed the induction of lytic replication, which correlated with decreased p-JNK expression levels (Fig. 6D). Taken together, these results suggest that extracellular HMGB1 induces phosphorylation of JNK in KSHV-producing cells, which is associated with enhanced lytic replication of KSHV.

**HMGB1 knockout attenuates virion production.** To investigate whether virion production is affected by HMGB1, the virus concentrate was collected from WT and *HMGB1* KO iSLK BAC16 cells maintained under the same culture conditions as those in

the experiments described above (equal number of seeded cells and the same volume of culture medium). The viral proteins from each concentrated virus sample were then analyzed by Western blotting (Fig. 7A). The abundance of KSHV envelope glycoproteins, such as K8.1 (32) and gB (33), was lower in the viruses from *HMGB1* KO cells than those from WT cells. The amount of the KSHV tegument protein ORF45 (34) was also lower in viruses produced in *HMGB1* KO cells.

In addition, we analyzed the number of KSHV genome copies in the collected virus samples using qPCR (Fig. 7B). As expected, the viral copy number was significantly lower in the viruses from *HMGB1* KO cells than in those from WT cells. Next, we infected human umbilical vein endothelial cells (HUVECs) with equal volumes of viruses from WT and *HMGB1* KO cells. KSHV BAC16 cells were designed to express GFP following KSHV infection of host cells (35). Therefore, infectivity can be monitored by measuring the GFP expression of infected cells. Using fluorescence microscopy, we detected significantly more GFP-expressing cells in the HUVECs infected with KSHV from WT cells than those infected with KSHV from *HMGB1* KO cells (Fig. 7C). Similarly, the GFP expression, as analyzed by flow cytometry, in KSHV-infected cells was significantly higher in cells infected with KSHV from WT cells compared to KSHV from *HMGB1* KO cells (Fig. 7D and E). The mRNA expression of KSHV *ORF73* in HUVECs infected with KSHV from WT host cells was also higher than that in HUVECs infected with KSHV from *HMGB1* KO cells (Fig. 7F). At 3 h postinfection, whole genomic DNA was extracted from virus-infected cells, and qPCR was conducted with primers for KSHV *ORF26* (Fig. 7G). As expected, the total amount of viral DNA was significantly higher in HUVECs infected with KSHV from WT host cells than in HUVECs infected with KSHV from *HMGB1* KO cells, indicating the presence of more KSHV particles in HUVECs infected with virus samples from WT iSLK BAC16 cells than in virus samples from *HMGB1* KO iSLK BAC16 cells.

## DISCUSSION

Multiple cellular and environmental factors control a viral life cycle. HMGB1 was originally described as a DNA-binding nuclear protein regulating the transcription levels of various genes by exerting effects on chromosomal architecture (36). In the present study, we found that, regardless of the induction of lytic replication, HMGB1 was constitutively expressed in the KSHV-producing cell line iSLK BAC16. Intracellular HMGB1 was found to form complexes with various proteins, and the levels of HMGB1-interacting proteins changed during latent and lytic replication. Furthermore, we demonstrated that extracellular HMGB1 was present in the supernatant from iSLK BAC16 cell cultures, and its abundance increased following reactivation of lytic replication. Extracellular HMGB1 enhanced lytic replication, which had an association with increased phosphorylated JNK. Moreover, KO of *HMGB1* altered the expression levels of cellular and viral transcripts during both latent and lytic replication in KSHV-infected cells. The expression levels of viral genes in *HMGB1* KO iSLK BAC16 cells were particularly attenuated during lytic replication, which could be caused by impaired viral progeny production.

Several studies have indicated that nuclear HMGB1 affects the viral life cycle through interactions with viral proteins. For example, HMGB1 interacts with the adeno-associated virus Rep proteins, which stimulate Rep-mediated DNA cleavage activity (37). In the Epstein-Barr virus, HMGB1 stimulates the lytic transactivating protein, RTA, and ZEBRA (38, 39). Furthermore, HMGB1 has been shown to have a secondary role as a cytokine released or secreted from cells into the extracellular milieu, where they play a critical role in initiating inflammation as a damage-associated molecular pattern molecule (7). Many viruses, including herpes simplex virus 2, dengue virus, hepatitis C virus, respiratory syncytial virus, and Newcastle disease virus, have been reported to induce HMGB1 release from the virus-infected cells (19, 21, 22, 40, 41). Since extracellular HMGB1 can trigger an immune response in a microenvironment with immune cells, it is considered a key pathogenic molecule in virus-mediated inflammatory diseases (42). Although evidence has

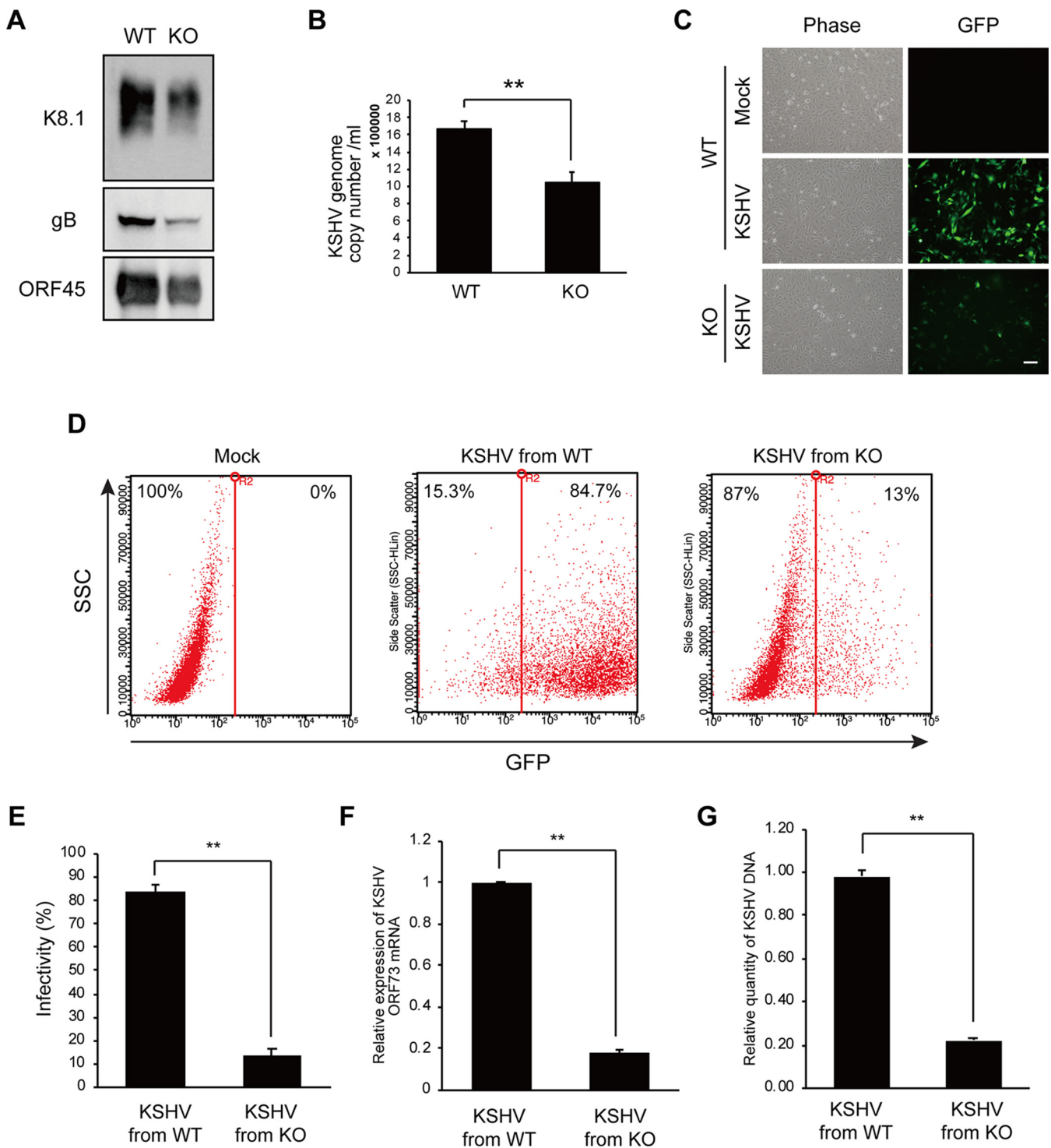


**FIG 7** Reduced KSHV production in *HMGB1* knockout iSLK BAC16 cells. (A) Western blotting of viral proteins in the samples of virions produced by wild-type (WT) and *HMGB1* knockout (KO) iSLK BAC16 cells. (B) Analysis of KSHV genome copy number in virions collected from WT and *HMGB1* KO iSLK BAC16 cells. (C) Microscopic images of human umbilical vein endothelial cells (HUVECs) infected by virions isolated from WT or *HMGB1* KO iSLK BAC16 cells. In the fluorescence microscopy images, the infected cells are displayed in green due to green fluorescent protein expression. The scale bar is 250 μm. (D and E) Flow cytometry analysis of the infectivity of KSHV virions obtained from WT and *HMGB1* KO iSLK BAC16 cells. A representative result (D) and statistical analysis (E) are illustrated. (F) Expression of KSHV *ORF73* mRNA in the HUVECs infected with KSHV virions isolated from WT or *HMGB1* KO iSLK BAC16 cells. After viral infection, total RNA was extracted and mRNA expression was analyzed by RT-qPCR. (G) Total KSHV DNA levels in the HUVECs infected with KSHV virions obtained from WT or *HMGB1* KO iSLK BAC16 cells. After infection, total genomic DNA was extracted, and KSHV DNA was quantified by qPCR using primers for KSHV *ORF26*. In all graphs, statistical significance of differences is indicated: \*\*,  $P < 0.01$ , Student's *t* test.

been provided for the effects of HMGB1 on the KSHV life cycle (15, 16), there have been no detailed studies on the effects of HMGB1 in KSHV-producing cells.

Additionally, HMGB1 may function as a cell-intrinsic factor affecting the viral life cycle through regulating the expression of host proteins. Indeed, a recent study demonstrated an epigenetic role for HMGB1 in regulating ACE2 expression, which is critical for entry of severe acute respiratory syndrome coronavirus 2 (SARS-CoV-2) (17). In this study, we established a CRISPR/Cas9-mediated *HMGB1* KO clone from KSHV-producing iSLK BAC16 cells. RNA-seq analysis demonstrated that *HMGB1* KO altered the expression of mRNAs and miRNAs. We also found that HMGB1 is a pleiotropic protein that participates in the formation of a nucleosomal complex with viral and cellular proteins, which was consistent with data from previous studies (15, 16), suggesting that such a complex could regulate viral gene expression. Additionally, through our RNA-seq and RT-qPCR analyses, we demonstrated that the expression of most viral mRNAs was suppressed in *HMGB1* KO clones during the induction of lytic replication (Fig. 3 and 4). Meanwhile, most KSHV viral genes were suppressed in *HMGB1* KO cells during lytic replication. Further, we confirmed that the mRNA expression of ORF72 and K13 in *HMGB1* KO cells was higher than that in WT cells under the same condition (Fig. 4A). Although the precise underlying mechanism responsible for the regulation of KSHV gene expression by HMGB1 remains unclear, we suspect that differentially expressed cellular miRNAs in *HMGB1* KO cells (Fig. 3) affect the expression of these viral genes. In fact, a previous study showed that the silencing of let-7 miRNA induces the mRNA transcription of KSHV ORF72 (43). Several studies have also reported that cellular miRNA regulates the expression of HMGB1 (44–46); however, to the best of our knowledge, our study is the first to demonstrate that the expression of various cellular miRNAs is regulated by HMGB1 (Fig. 3C). We are currently investigating the changes in miRNAs whose expression is induced in response to *HMGB1* KO and their implication in cells.

Considering that extracellular HMGB1 was detected in KSHV-producing iSLK BAC16 cells and that HMGB1 was found to activate multiple signaling pathways by interacting with surface receptors, we hypothesize that KSHV production is influenced indirectly by the HMGB1-mediated regulation of host gene expression. This notion is further supported by the fact that induction of KSHV lytic replication is affected by many cellular signaling pathways and depends on the expression of multiple genes (47). Specifically, we found that phosphorylation of JNK (p-JNK), a signaling protein activated by the interaction between RAGE and HMGB1 (31, 48), was suppressed in *HMGB1* KO cells and glycyrrhizin-treated WT cells during KSHV reactivation (Fig. 6). Previous studies have shown that p-JNK is associated with the lytic replication of KSHV (27, 28). We also identified a correlation between the expression of KSHV ORF50 and p-JNK. Taken together, these findings demonstrate that extracellular HMGB1 can regulate lytic replication through JNK signaling.

In conclusion, our results suggest that both intracellular and extracellular HMGB1 are associated with activation of the RTA promoter during reactivation through independent mechanisms. Of note, this is the first study to demonstrate the role of extracellular HMGB1 in the reactivation of KSHV. Thus, HMGB1 may function as a major cofactor in the reactivation of KSHV, which regulates the production of infectious virions in host cells. However, the precise function of the extracellular HMGB1 released from reactivated KSHV-infected cells in KS lesions remains unclear. Furthermore, because extracellular HMGB1 has diverse immunological roles that affect cytokine production, cell proliferation, chemotaxis, angiogenesis, and cell differentiation (49), it may serve as a modulator of the microenvironment for KSHV-infected cells. Further studies are necessary to clarify whether extracellular HMGB1 has any role in the pathogenesis of KSHV-associated diseases, such as inflammation and the development of Kaposi's sarcoma.

## MATERIALS AND METHODS

**Cell culture and reagents.** iSLK BAC16 cells (35) were cultured in high-glucose Dulbecco's modified Eagle's medium (WelGene, Gyeongsan, South Korea) supplemented with 10% fetal bovine serum (FBS;

GenDEPOT, Katy, TX), 1% antibiotic-antimycotic (Thermo Fisher Scientific, Inc., Waltham, MA), Geneticin (250  $\mu$ g/ml; Thermo Fisher Scientific), and puromycin (1  $\mu$ g/ml; Thermo Fisher Scientific). BAC16 contains a cassette encoding GFP to monitor infectivity. iSLK BAC16 cells were selected with hygromycin to achieve stable latent infection. HUVECs were purchased from PromoCell (Heidelberg, Germany) and cultured in endothelial cell growth medium 2 (PromoCell) containing cell growth supplement. All cells were incubated or maintained in a humidified atmosphere containing 95% air and 5% CO<sub>2</sub> at 37°C. Glycyrrhizin was purchased from Sigma-Aldrich (St. Louis, MO).

**Western blotting.** Total protein was collected using cell lysis buffer containing 20 mM Tris-HCl (pH 6.8), 150 mM NaCl, 10 mM EDTA, 1 mM EGTA, 1% Triton X-100, or radioimmunoprecipitation assay buffer (LPS Solution, Daejeon, South Korea) supplemented with 0.1 mM NaF, 0.1 mM phenylmethylsulfonyl fluoride, 1 mM beta-glycerophosphate, and 0.1 mM sodium orthovanadate. The protein suspension was incubated at 4°C for 15 min and then centrifuged at 14,000  $\times g$  for 15 min at 4°C. The supernatant was collected, and the protein concentration was measured by the bicinchoninic acid assay (Pierce, Rockford, IL). Proteins were separated in 10% and 15% sodium dodecyl sulfate-polyacrylamide gels and transferred onto nitrocellulose membranes. The membranes were blocked at 4°C overnight on a rocker with 5% skim milk in a 0.1% TBST solution (1  $\times$  Tris-buffered saline with 0.1% Tween 20). Primary antibodies were diluted in 5% bovine serum albumin (BSA) in TBST and reacted with samples by rocking at 4°C overnight. Secondary antibodies were diluted in 5% skim milk-TBST and reacted on a rocker at room temperature for 1 h. Immunolabeled proteins were visualized using Clarity Western ECL substrate (Bio-Rad Laboratories, Hercules, CA) and a Chemidoc touch imaging system (Bio-Rad Laboratories) or autoradiography film. Immunodetection was performed using rabbit antibodies against HMGB1 (Abcam, Cambridge, MA), HHV8 ORF50, total p38 MAPK, phosphorylated p38 MAPK (Thr180/Tyr182), total JNK1/2, and phosphorylated ERK (Thr202/Tyr204) (all from Bioss, Woburn, MA); mouse antibodies against  $\beta$ -actin (Sigma), HDAC1, HHV-8 K8.1A/B, HHV8 ORF57, and phosphorylated JNK (Thr183/Tyr185) (all Santa Cruz, Santa Cruz, CA); and a rat antibody against HHV8 LNA (Abcam). Secondary antibodies included horseradish peroxidase (HRP)-conjugated goat anti-mouse IgG (Bethyl, Montgomery, TX), HRP-conjugated goat anti-rabbit IgG (Bethyl), and HRP-conjugated goat anti-rat IgG (Bethyl). Quantification of protein bands in Western blot analysis was performed using Image Lab 6.1 software (Bio-Rad).

**Immunofluorescence assay.** Cell monolayers were fixed in 4% paraformaldehyde for 30 min at room temperature and washed with phosphate-buffered saline (PBS). The fixed cells were permeabilized with 0.25% Triton X-100-PBS for 15 min at room temperature. After blocking with 3% BSA-PBS for 30 min at 4°C, the samples were incubated for 1 h at room temperature with a rabbit monoclonal anti-HMGB1 antibody (Abcam) in 3% BSA-TBST. After washing with PBS containing 0.05% Tween 20, the samples were incubated for 30 min at room temperature with an Alexa Fluor 568-conjugated anti-rabbit IgG antibody (Thermo Fisher Scientific) in PBS containing 3% BSA. Nuclei were stained for 1 min using a 500-ng/ml 4',6-diamidino-2-phenylindole (DAPI) solution in PBS. Samples were mounted in FluorSave reagent (Sigma). Images were obtained using a Nikon Eclipse E400 microscope (Nikon, Tokyo, Japan) and Nikon digital suite DS-U2 (Nikon) and analyzed using NIS element F (Nikon).

**Establishment of an HMGB1 knockout clone using the CRISPR/Cas9 system.** For synthetic gRNA for HMGB1, crRNA (catalog number A35509, chr13:30463559~30463537), and tracrRNA were purchased from Thermo Fisher Scientific. The CRISPR guide RNA annealing condition followed the Invitrogen TrueGuide. Briefly, crRNA and tracrRNA were dissolved in 1  $\times$  TE buffer to a final concentration of 100  $\mu$ M. The mixture was synthesized into gRNA in a Bio-Rad CFX 96 thermocycler using the following steps: (i) 95°C for 5 min; (ii) 95°C to 78°C at a ramp rate of  $-2^{\circ}\text{C/s}$ ; (iii) 78°C for 10 min; (iv) 78°C to 25°C at a ramp rate of  $-0.1^{\circ}\text{C/s}$ ; and (v) 25°C for 5 min. CRISPR RNA mixture and TrueCut Cas9 protein v2 were transfected into iSLK BAC16 using the Lipofectamine CRISPRMAX Cas9 transfection reagent (Thermo Fisher Scientific) according to the manufacturer's recommendations. Both gRNA and Cas9 protein were added at a final concentration of 0.15  $\mu$ M. After 3 days of transfection, the cells were detached from the culture well, and their number was adjusted to eight per 1 ml. The cells then were seeded into 96-well plates at 100  $\mu$ l/well. The plates were scanned for cell growth to find wells with only a single colony growing. The cells of such colonies were dissociated using trypsin treatment and cultured in a new, larger culture dish. After collecting a protein extract for each clone, KO of HMGB1 was confirmed through Western blotting.

**qPCR analysis for the identification of mutations.** Genomic DNA from cultured cells was collected using the DNeasy blood and tissue kit (Qiagen, Valencia, CA). To confirm differences in the PCR amplification efficiency of HMGB1 by CRISPR/Cas9 knockout, we designed two pairs of primers; the first was designed to bind outside the Cas9 target sequences (primer F, 5'-GAAAAATAACTAAACATGGGCAA-3'; primer R, 5'-CCACTACGAGAATGCCAA-3'), and the other flanked the Cas9 target sequences (primer S, 5'-TTCTAAGAAGTGCTCAGAG-3') (Fig. 2A). Before performing qPCR, we ran an ordinary PCR to obtain DNA fragments using the outside primers for qPCR and cloning. PCR was performed using Solg 2  $\times$  Taq PCR premix (Solgent, Daejeon, South Korea) according to the manufacturer's instructions (denaturation at 95°C for 5 min, amplification for 35 cycles of 95°C for 30 s, 60°C for 30 s, and 72°C for 30 s, and final extension at 72°C for 5 min). The amplified fragments were quantified and adjusted to equal amounts for subsequent qPCR. TB green fast qPCR mix (TaKaRa, Kyoto, Japan) was used for melting curve analysis using qPCR. qPCR cycling conditions were set to denaturation at 95°C for 30 s, with amplification for 40 cycles (95°C for 5 s and 60°C for 30 s). After amplification of the PCR product, melting curve analysis was performed between 65°C and 95°C in 0.5°C increments. To confirm the PCR product, we loaded it on 2% agarose-TBE gel and confirmed the band.

**Sequencing analysis of the HMGB1 KO clone through T-vector cloning.** Using the TOPcloner TA kit (Enzymatics, Daejeon, South Korea), the PCR products were inserted into the vector and transformed

into *Escherichia coli* DH5 $\alpha$  according to the manufacturer's recommendations. The transformed *E. coli* cells were cultured on an LB agar plate containing 40  $\mu$ g/ml ampicillin. Recombinant clones were recovered and cultured in Terrific broth (Sigma) containing 40  $\mu$ g/ml ampicillin at 37°C overnight. Plasmids were then isolated using a Plasmid minikit (MGmed, Seoul, South Korea). Sequencing analysis was conducted at Bionics (Seoul, South Korea). First, PCR was performed using the BigDye Terminator v3.1 cycle sequencing kit (Applied Biosystems, Waltham, MA). After the PCR product was cleaned, the sequences were analyzed using an Applied Biosystems 3730XL DNA analyzer (Applied Biosystems). M13F (5'-GTAAACGACGGCCAG-3') and M13R (5'-CAGGAACAGCTATGAC-3'), included in the TOPcloner TA kit, were used as sequencing primers. Reference sequences (*Homo sapiens* chromosome 13, GRCh38.p13 primary assembly 30,456,704 to 30,617,597; NCBI accession no. [NC\\_000013.11](#)) and analyzed sequences were aligned using SnapGene v5.2.4 (GSL Biotech LLC, CA, USA).

**WST-1 cell viability assay.** Cell proliferation was analyzed using the WST-1 cell proliferation reagent (Roche, Basel, Switzerland). WT or *HMGB1* KO iSLK BAC16 cells ( $5 \times 10^3$ ) were seeded into 96-well culture plates (SPL Life Science, Pocheon, South Korea) and incubated for 1 to 3 days, followed by treatment with WST-1 (1:10 dilution) for 90 min at 37°C and 5% CO<sub>2</sub>. Absorbance at 450 nm was analyzed using a microplate reader (Molecular Devices, Silicon Valley, CA).

**TruSeq stranded mRNA sample preparation.** Total RNA was extracted from WT and *HMGB1* KO iSLK BAC16 cells using a RiboSpin II kit (GeneAll Biotechnology, Seoul, South Korea) according to the manufacturer's instructions. RNA concentration and integrity were evaluated using Quant-IT RiboGreen (Thermo Fisher Scientific) and TapeStation RNA ScreenTape (Agilent Technologies, Palo Alto, CA), respectively. *Homo sapiens* and human herpesvirus transcriptome sequencing was performed according to the manufacturer's protocol (Illumina, Inc., San Diego, CA). A library was independently prepared with 1  $\mu$ g of total RNA for each sample using an Illumina TruSeq stranded mRNA sample prep kit (Illumina, Inc.). The first step in the workflow involved purifying the poly(A)-containing mRNA molecules using poly(T)-attached magnetic beads. Following purification, the mRNA was fragmented into small pieces in the presence of solutions of divalent cations at an elevated temperature. The cleaved RNA fragments were copied into first-strand cDNA using SuperScript II reverse transcriptase (Thermo Fisher Scientific) and random primers. This was followed by second-strand cDNA synthesis using DNA polymerase I, RNase H, and dUTP. These cDNA fragments then went through the end repair process, the addition of a single A base, and ligation of the adapters. The products were then purified and enriched with PCR to create the final cDNA library. The libraries were quantified using KAPA library quantification kits for Illumina Sequencing platforms according to the qPCR quantification protocol guide (Sigma) and qualified using the TapeStation D1000 ScreenTape (Agilent Technologies). Indexed libraries were then submitted to an Illumina NovaSeq (Illumina, Inc.), and paired-end ( $2 \times 100$  bp) sequencing was performed by Macrogen Incorporated (Daejeon, South Korea).

**mRNA-seq and data analysis of *Homo sapiens* and human herpesvirus 8 transcriptome sequencing results.** The raw reads from the sequencer were preprocessed to remove low-quality and adapter sequences before analysis. The processed reads then were aligned to the *Homo sapiens* (GRCh37) and human herpesvirus 8 strain (GK18) builds using bowtie, which utilizes two types of indexes for alignment (a global, whole-genome index and tens of thousands of small local indices). These two types of indices were constructed using the same Ferragina-Manzini index based on the Burrows-Wheeler transform as Bowtie2. Transcript assembly and abundance estimation were performed using StringTie (<https://ccb.jhu.edu/software/stringtie/>). Genes with one less than zero read count values in the samples were excluded. To facilitate log<sub>2</sub> transformation, 1 was added to each read count value of filtered genes. Filtered data were log<sub>2</sub> transformed and subjected to trimmed mean of M values normalization. Statistical significance of the differences in expression levels was determined by analyzing fold change data with exactTest in edgeR, with the null hypothesis assuming no difference between groups. False discovery rate was controlled by adjusting *P* values using the Benjamini-Hochberg algorithm. For the differentially expressed gene set, hierarchical clustering analysis was performed using complete linkage and Euclidean distance as measures of similarity. Gene enrichment, functional annotation analysis, and pathway analysis for significantly differentially expressed genes were performed based on Gene Ontology ([www.geneontology.org](http://www.geneontology.org)). Variations in gene expression levels were analyzed using Morpheus (<https://software.broadinstitute.org/morpheus/>). Furthermore, the bar graph summary as well as the pathway and process enrichment analysis were performed using the Metascape gene annotation and analysis resource (<http://metascape.org>).

**RT-qPCR.** Total RNA was collected from cultured cells using a RiboSpin II RNA isolation kit (GeneAll Biotechnology). Reverse transcription of the total RNA to synthesize cDNA was performed using TaKaRa RT Master Mix II (TaKaRa, Shiga, Japan). Quantitative real-time reverse transcription-PCR (RT-qPCR) was performed using TaKaRa SYBR FAST qPCR mix (TaKaRa). The cycling conditions were 95°C for 30 s, 40 cycles of 95°C for 5 s, and 60°C for 10 s. The specificity of the amplified products was confirmed by melting curve analysis. All samples were processed in triplicate, and gene expression levels were normalized to the gene expression level of glyceraldehyde 3-phosphate dehydrogenase (*GAPDH*). The following primers were used in this study: ORF50s, 5'-TGG TGG AAG ATG TGT GCA TT-3', and ORF50as, 5'-CTC CGT GAG GAT CCG AAT AA-3', for KSHV *ORF50*; ORF65s, 5'-ACT ATC TCG TGT TCT TAA TTG C-3', and ORF65as, 5'-ATG ATC CCG CCT TTG AAT-3', for KSHV *ORF65*; ORF73s, 5'-CCA GGA AGT CCC ACA GTG TT-3', and ORF73as, 5'-AGA CAC AGG ATG GGA TGG AG-3', for KSHV *ORF73*; *GAPDH*s, 5'-GGT ATC GTG GAA GGA CTC-3', and *GAPDH*as, 5'-GTA GAG GCA GGG ATG ATG-3', for *GAPDH*. The primers were synthesized by Genotech (Daejeon, South Korea).

**Immunoprecipitation analysis.** Cell lysates were incubated with a rabbit anti-HMGB1 antibody (Abcam) or a rabbit monoclonal antibody IgG XP control (Cell Signaling Technology, Danvers, MA)

overnight at 4°C, and the antigen-antibody complexes were precipitated with Pierce protein A/G agarose (Thermo Fisher Scientific) for 2 h at room temperature. The immunoprecipitated complexes were cleared and analyzed by Western blotting as described above.

**Production of KSHV and infection of HUVECs.** To induce lytic replication, iSLK BAC16 cells were treated for 48 h with 1.2 mM sodium butyrate (Sigma) and 50 µg/ml doxycycline (Sigma). The culture medium was collected, and cell debris was removed from the culture supernatant by centrifugation at  $2,000 \times g$  for 10 min at 4°C. After that, the supernatant was centrifuged again at  $100,000 \times g$  for 1 h at 4°C. The virus pellet was resuspended in cold PBS, and the virus stock was stored at -80°C until use. The prepared KSHV stock from WT or HMGB1 KO iSLK BAC16 cells was used for infection of HUVECs with OptiMEM containing 5 µg/ml Polybrene (Santa Cruz). Infection of HUVECs with KSHV was performed by centrifugation at  $2,000 \times g$  for 1 h at 25°C. After centrifugation, the medium was changed to endothelial cell growth medium 2 (PromoCell), and HUVECs were then cultured overnight at 37°C in an atmosphere containing 95% air and 5% CO<sub>2</sub>.

**Quantification of the relative copy number of KSHV genomic DNA by qPCR.** KSHV samples extracted from WT or HMGB1 KO iSLK BAC16 cells were treated with DNase I (Enzynomics, Daejeon, South Korea) at 37°C for 10 min to remove DNA outside virion particles. To inactivate DNase I, DNase I-treated virus was heated at 75°C for 10 min. The viral DNA was isolated by a DNeasy blood & tissue DNA prep kit (Qiagen) according to the manufacturer's instructions. Real-time PCR was performed using TaKaRa SYBR fast qPCR Mix (TaKaRa). The cycling conditions were 95°C for 30 s, 40 cycles of 95°C for 5 s, and 60°C for 10 s. The specificity of the amplified products was confirmed by melting curve analysis. For the detection of the KSHV *ORF26* gene, 5'-GGA GAT TGC CAC CGT TTA-3' (forward) and 5'-ACT GCA TAA TTT GGA TGT AGT C-3' (reverse) were used as primers.

**Flow cytometry analysis of KSHV infectivity.** The cells infected with the recombinant KSHV BAC16 containing the gene encoding GFP were detached with trypsin-EDTA solution (Sigma) and resuspended in PBS supplemented with 1% FBS. KSHV infectivity was analyzed by the expression of GFP measured using a Guava easyCyte flow cytometer (Luminex Corporation, Austin, TX) and analyzed using InCyte 3.1 software (Luminex Corporation).

**Statistical analysis.** Each experiment was performed at least three times independently, and representative results are shown. In the graphs, the results are presented as the means  $\pm$  standard deviations. Two-tailed Student's *t* test was used to compare data between the different groups. For more than two groups, one-way analysis of variance (ANOVA) was used. Data were considered significantly different at a *P* value of <0.05. Statistical significance of differences was indicated with asterisks: \*, *P* < 0.05; \*\*, *P* < 0.01.

**Data availability.** The transcriptomes of wild-type (WT) and HMGB1 knockout (KO) cells were analyzed by mRNA-seq, and the data were deposited in the Gene Expression Omnibus under accession numbers GSE157275 and GSE172275.

## ACKNOWLEDGMENTS

This research was supported by the Mid-Career Research Program through the National Research Foundation of Korea (NRF), project number NRF-2019R1A2C2083947, to M.-S.L.

We have no competing interests to declare.

## REFERENCES

- Goncalves PH, Ziegelbauer J, Uldrick TS, Yarchoan R. 2017. Kaposi sarcoma herpesvirus-associated cancers and related diseases. *Curr Opin HIV AIDS* 12:47–56. <https://doi.org/10.1097/COH.0000000000000330>.
- Zhang F, Liang D, Lin X, Zou Z, Sun R, Wang X, Liang X, Kaye KM, Lan K. 2019. NDRG1 facilitates the replication and persistence of Kaposi's sarcoma-associated herpesvirus by interacting with the DNA polymerase clamp PCNA. *PLoS Pathog* 15:e1007628. <https://doi.org/10.1371/journal.ppat.1007628>.
- Zou Z, Meng Z, Ma C, Liang D, Sun R, Lan K. 2017. Guanylate-binding protein 1 inhibits nuclear delivery of kaposi's sarcoma-associated herpesvirus virions by disrupting formation of actin filament. *J Virol* 91:e00632-17. <https://doi.org/10.1128/JVI.00632-17>.
- Guito J, Lukac DM. 2015. KSHV reactivation and novel implications of protein isomerization on lytic switch control. *Viruses* 7:72–109. <https://doi.org/10.3390/v7010072>.
- Davis ZH, Verschuere E, Jang GM, Kleffman K, Johnson JR, Park J, Von Dollen J, Maher MC, Johnson T, Newton W, Jäger S, Shales M, Horner J, Hernandez RD, Krogan NJ, Glaunsinger BA. 2015. Global mapping of herpesvirus-host protein complexes reveals a transcription strategy for late genes. *Mol Cell* 57:349–360. <https://doi.org/10.1016/j.molcel.2014.11.026>.
- Einck L, Bustin M. 1985. The intracellular distribution and function of the high mobility group chromosomal proteins. *Exp Cell Res* 156:295–310. [https://doi.org/10.1016/0014-4827\(85\)90539-7](https://doi.org/10.1016/0014-4827(85)90539-7).
- Sims GP, Rowe DC, Rietdijk ST, Herbst R, Coyle AJ. 2010. HMGB1 and RAGE in inflammation and cancer. *Annu Rev Immunol* 28:367–388. <https://doi.org/10.1146/annurev.immunol.021908.132603>.
- Luan ZG, Zhang H, Yang PT, Ma XC, Zhang C, Guo RX. 2010. HMGB1 activates nuclear factor- $\kappa$ B signaling by RAGE and increases the production of TNF- $\alpha$  in human umbilical vein endothelial cells. *Immunobiology* 215:956–962. <https://doi.org/10.1016/j.imbio.2009.11.001>.
- Yuan S, Liu Z, Xu Z, Liu J, Zhang J. 2020. High mobility group box 1 (HMGB1): a pivotal regulator of hematopoietic malignancies. *J Hematol Oncol* 13:91. <https://doi.org/10.1186/s13045-020-00920-3>.
- Li R, Zou X, Huang H, Yu Y, Zhang H, Liu P, Pan S, Ouyang Y, Shang Y. 2020. HMGB1/PI3K/Akt/mTOR signaling participates in the pathological process of acute lung injury by regulating the maturation and function of dendritic cells. *Front Immunol* 11:1104. <https://doi.org/10.3389/fimmu.2020.01104>.
- Zhu X, Sun L, Wang Y. 2016. High mobility group box 1 (HMGB1) is upregulated by the Epstein-Barr virus infection and promotes the proliferation of human nasopharyngeal carcinoma cells. *Acta Otolaryngol* 136:87–94. <https://doi.org/10.3109/00016489.2015.1082192>.
- Kimura R, Mori N. 2014. Abundant expression of HMGB1 in human T-cell lymphotropic virus type I-infected T-cell lines and high plasma levels of HMGB1 in patients with adult T-cell leukemia. *Oncol Lett* 7:1239–1242. <https://doi.org/10.3892/ol.2014.1851>.
- Fu S, Wang J, Hu X, Zhou RR, Fu Y, Tang D, Kang R, Huang Y, Sun L, Li N, Fan XG. 2018. Crosstalk between hepatitis B virus X and high-mobility group box 1 facilitates autophagy in hepatocytes. *Mol Oncol* 12:322–338. <https://doi.org/10.1002/1878-0261.12165>.
- Moisy D, Avilov SV, Jacob Y, Laoide BM, Ge X, Baudin F, Naffakh N, Jestin JL. 2012. HMGB1 protein binds to influenza virus nucleoprotein and

- promotes viral replication. *J Virol* 86:9122–9133. <https://doi.org/10.1128/JVI.00789-12>.
15. Song MJ, Hwang S, Wong W, Round J, Martinez-Guzman D, Turpaz Y, Liang J, Wong B, Johnson RC, Carey M, Sun R. 2004. The DNA architectural protein HMGB1 facilitates RTA-mediated viral gene expression in gamma-2 herpesviruses. *J Virol* 78:12940–12950. <https://doi.org/10.1128/JVI.78.23.12940-12950.2004>.
  16. Harrison SM, Whitehouse A. 2008. Kaposi's sarcoma-associated herpesvirus (KSHV) Rta and cellular HMGB1 proteins synergistically transactivate the KSHV ORF50 promoter. *FEBS Lett* 582:3080–3084. <https://doi.org/10.1016/j.febslet.2008.07.055>.
  17. Wei J, Alfajaro MM, DeWeirdt PC, Hanna RE, Lu-Culligan WJ, Cai WL, Strine MS, Zhang SM, Graziano VR, Schmitz CO, Chen JS, Mankowski MC, Filler RB, Ravindra NG, Gasque V, de Miguel FJ, Patil A, Chen H, Oguntuyo KY, Abriola L, Surovtseva YV, Orchard RC, Lee B, Lindenbach BD, Politi K, van Dijk D, Kadoch C, Simon MD, Yan Q, Doench JG, Wilen CB. 2021. Genome-wide CRISPR screens reveal host factors critical for SARS-CoV-2 infection. *Cell* 184:76–91. <https://doi.org/10.1016/j.cell.2020.10.028>.
  18. Saïdi H, Melki MT, Gougeon ML. 2008. HMGB1-dependent triggering of HIV-1 replication and persistence in dendritic cells as a consequence of NK-DC cross-talk. *PLoS One* 3:e3601. <https://doi.org/10.1371/journal.pone.0003601>.
  19. Borde C, Barnay-Verdier S, Gaillard C, Hocini H, Maréchal V, Gozlan J. 2011. Stepwise release of biologically active HMGB1 during HSV-2 infection. *PLoS One* 6:e16145. <https://doi.org/10.1371/journal.pone.0016145>.
  20. Gustafsson R. 2021. Human herpesvirus 6A induces dendritic cell death and HMGB1 release without virus replication. *Pathogens* 10:57. <https://doi.org/10.3390/pathogens10010057>.
  21. Ong SP, Lee LM, Leong YF, Ng ML, Chu JJ. 2012. Dengue virus infection mediates HMGB1 release from monocytes involving PCAF acetylase complex and induces vascular leakage in endothelial cells. *PLoS One* 7: e41932. <https://doi.org/10.1371/journal.pone.0041932>.
  22. Qu Y, Zhan Y, Yang S, Ren S, Qiu X, Rehman ZU, Tan L, Sun Y, Meng C, Song C, Yu S, Ding C. 2018. Newcastle disease virus infection triggers HMGB1 release to promote the inflammatory response. *Virology* 525:19–31. <https://doi.org/10.1016/j.virol.2018.09.001>.
  23. Aneja KK, Yuan Y. 2017. Reactivation and lytic replication of Kaposi's sarcoma-associated herpesvirus: an update. *Front Microbiol* 8:613. <https://doi.org/10.3389/fmicb.2017.00613>.
  24. Lu F, Zhou J, Wiedmer A, Madden K, Yuan Y, Lieberman PM. 2003. Chromatin remodeling of the Kaposi's sarcoma-associated herpesvirus ORF50 promoter correlates with reactivation from latency. *J Virol* 77:11425–11435. <https://doi.org/10.1128/jvi.77.21.11425-11435.2003>.
  25. Shamay M, Liu J, Li R, Liao G, Shen L, Greenway M, Hu S, Zhu J, Xie Z, Ambinder RF, Qian J, Zhu H, Hayward SD. 2012. A protein array screen for Kaposi's sarcoma-associated herpesvirus LANA interactors links LANA to TIP60, PP2A activity, and telomere shortening. *J Virol* 86:5179–5191. <https://doi.org/10.1128/JVI.00169-12>.
  26. Harris HE, Andersson U, Pisetsky DS. 2012. HMGB1: a multifunctional alarmin driving autoimmune and inflammatory disease. *Nat Rev Rheumatol* 8:195–202. <https://doi.org/10.1038/nrrheum.2011.222>.
  27. Xie J, Ajibade AO, Ye F, Kuhne K, Gao SJ. 2008. Reactivation of Kaposi's sarcoma-associated herpesvirus from latency requires MEK/ERK, JNK and p38 multiple mitogen-activated protein kinase pathways. *Virology* 371:139–154. <https://doi.org/10.1016/j.virol.2007.09.040>.
  28. Pan H, Xie J, Ye F, Gao SJ. 2006. Modulation of Kaposi's sarcoma-associated herpesvirus infection and replication by MEK/ERK, JNK, and p38 multiple mitogen-activated protein kinase pathways during primary infection. *J Virol* 80:5371–5382. <https://doi.org/10.1128/JVI.02299-05>.
  29. Ford PW, Bryan BA, Dyson OF, Weidner DA, Chintalgattu V, Akula SM. 2006. Raf/MEK/ERK signalling triggers reactivation of Kaposi's sarcoma-associated herpesvirus latency. *J Gen Virol* 87:1139–1144. <https://doi.org/10.1099/vir.0.81628-0>.
  30. Bangert A, Andrassy M, Muller AM, Bockstahler M, Fischer A, Volz CH, Leib C, Goser S, Korkmaz-Icoz S, Zittrich S, Jungmann A, Lasitschka F, Pfitzer G, Muller OJ, Katus HA, Kaya Z. 2016. Critical role of RAGE and HMGB1 in inflammatory heart disease. *Proc Natl Acad Sci U S A* 113:E155–64. <https://doi.org/10.1073/pnas.1522288113>.
  31. Wu X, Mi Y, Yang H, Hu A, Zhang Q, Shang C. 2013. The activation of HMGB1 as a progression factor on inflammation response in normal human bronchial epithelial cells through RAGE/JNK/NF-kappaB pathway. *Mol Cell Biochem* 380:249–257. <https://doi.org/10.1007/s11010-013-1680-0>.
  32. Luna RE, Zhou F, Baghian A, Chouljenko V, Forghani B, Gao SJ, Kousoulas KG. 2004. Kaposi's sarcoma-associated herpesvirus glycoprotein K8.1 is dispensable for virus entry. *J Virol* 78:6389–6398. <https://doi.org/10.1128/JVI.78.12.6389-6398.2004>.
  33. Krishnan HH, Sharma-Walia N, Zeng L, Gao SJ, Chandran B. 2005. Envelope glycoprotein gB of Kaposi's sarcoma-associated herpesvirus is essential for egress from infected cells. *J Virol* 79:10952–10967. <https://doi.org/10.1128/JVI.79.17.10952-10967.2005>.
  34. Zhu FX, Yuan Y. 2003. The ORF45 protein of Kaposi's sarcoma-associated herpesvirus is associated with purified virions. *J Virol* 77:4221–4230. <https://doi.org/10.1128/jvi.77.7.4221-4230.2003>.
  35. Brulois KF, Chang H, Lee AS, Ensser A, Wong LY, Toth Z, Lee SH, Lee HR, Myoung J, Ganem D, Oh TK, Kim JF, Gao SJ, Jung JU. 2012. Construction and manipulation of a new Kaposi's sarcoma-associated herpesvirus bacterial artificial chromosome clone. *J Virol* 86:9708–9720. <https://doi.org/10.1128/JVI.01019-12>.
  36. Javaherian K, Liu JF, Wang JC. 1978. Nonhistone proteins HMGI and HMGI2 change the DNA helical structure. *Science* 199:1345–1346. <https://doi.org/10.1126/science.628842>.
  37. Costello E, Saudan P, Winocour E, Pizer L, Beard P. 1997. High mobility group chromosomal protein 1 binds to the adeno-associated virus replication protein (Rep) and promotes Rep-mediated site-specific cleavage of DNA, ATPase activity and transcriptional repression. *EMBO J* 16:5943–5954. <https://doi.org/10.1093/emboj/16.19.5943>.
  38. Mitsouras K, Wong B, Arayata C, Johnson RC, Carey M. 2002. The DNA architectural protein HMGB1 displays two distinct modes of action that promote enhanceosome assembly. *Mol Cell Biol* 22:4390–4401. <https://doi.org/10.1128/MCB.22.12.4390-4401.2002>.
  39. Ellwood KB, Yen YM, Johnson RC, Carey M. 2000. Mechanism for specificity by HMGI-1 in enhanceosome assembly. *Mol Cell Biol* 20:4359–4370. <https://doi.org/10.1128/MCB.20.12.4359-4370.2000>.
  40. Hosakote YM, Brasier AR, Casola A, Garofalo RP, Kurosky A. 2016. Respiratory syncytial virus infection triggers epithelial HMGB1 release as a damage-associated molecular pattern promoting a monocytic inflammatory response. *J Virol* 90:9618–9631. <https://doi.org/10.1128/JVI.01279-16>.
  41. Yu R, Yang D, Lei S, Wang X, Meng X, Xue B, Zhu H. 2015. HMGB1 promotes hepatitis C virus replication by interaction with stem-loop 4 in the viral 5' untranslated region. *J Virol* 90:2332–2344. <https://doi.org/10.1128/JVI.02795-15>.
  42. Andersson U, Ottestad W, Tracey KJ. 2020. Extracellular HMGB1: a therapeutic target in severe pulmonary inflammation including COVID-19? *Mol Med* 26:42. <https://doi.org/10.1186/s10020-020-00172-4>.
  43. Zhang JX, Tan XH, Yuan Z, Li YH, Qi Y, Nan X, Qi MJ, Gao H, Lian FZ, Yang L. 2016. Let-7 miRNA silencing promotes Kaposi's sarcoma-associated herpesvirus lytic replication via activating mitogen-activated protein kinase zeta kinase kinase 4 and its downstream factors. *Zhonghua Zhong Liu Za Zhi* 38:485–491.
  44. Abdulla OA, Neamah W, Sultan M, Chatterjee S, Singh N, Nagarkatti M, Nagarkatti P. 2021. AhR ligands differentially regulate miRNA-132 which targets HMGB1 and to control the differentiation of Tregs and Th-17 cells during delayed-type hypersensitivity response. *Front Immunol* 12:635903. <https://doi.org/10.3389/fimmu.2021.635903>.
  45. Lv S, Guan M. 2018. miRNA-1284, a regulator of HMGB1, inhibits cell proliferation and migration in osteosarcoma. *Biosci Rep* 38:BSR20171675. <https://doi.org/10.1042/BSR20171675>.
  46. Zhang C, Ge S, Hu C, Yang N, Zhang J. 2013. miRNA-218, a new regulator of HMGB1, suppresses cell migration and invasion in non-small cell lung cancer. *Acta Biochim Biophys Sin* 45:1055–1061. <https://doi.org/10.1093/abbs/gct109>.
  47. Purushothaman P, Uppal T, Verma SC. 2015. Molecular biology of KSHV lytic reactivation. *Viruses* 7:116–153. <https://doi.org/10.3390/v7010116>.
  48. Kim SW, Lim CM, Kim JB, Shin JH, Lee S, Lee M, Lee JK. 2011. Extracellular HMGB1 released by NMDA treatment confers neuronal apoptosis via RAGE-p38 MAPK/ERK signaling pathway. *Neurotox Res* 20:159–169. <https://doi.org/10.1007/s12640-010-9231-x>.
  49. Andersson U, Tracey KJ. 2011. HMGB1 is a therapeutic target for sterile inflammation and infection. *Annu Rev Immunol* 29:139–162. <https://doi.org/10.1146/annurev-immunol-030409-101323>.